antioxidants

MDPI

Article

Multiblock Integrative Modelling of New Zealand Monofloral Honeys: Mapping the Multi-Constituent Drivers of Antioxidant and Anti-Tyrosinase Activity

Rushan Lakshitha [1], Adrian Owens [1], Kevin Kantono [1], Thao T. Le [1], Swapna Gannabathula [2] and Nazimah Hamid [1,*]

[1] AUT Centre for Future Foods, School of Science, Faculty of Health and Environment Sciences, Auckland University of Technology, Private Bag 92006, Auckland 1010, New Zealand; ycn4788@autuni.ac.nz (R.L.); adrian.owens@aut.ac.nz (A.O.); kkantono@aut.ac.nz (K.K.); thao.le@aut.ac.nz (T.T.L.)

[2] The Experiment Company, Auckland 1052, New Zealand; swapna.nz@gmail.com

* Correspondence: nazimah.hamid@aut.ac.nz; Tel.: +64-9-9219999 (ext. 6453); Fax: +64-9-9219627

Abstract

Honey bioactivity is a multi-constituent property often oversimplified by single-marker analysis. This study applied an exploratory multiblock integrative framework to map the systems-level architecture of bioactivity in New Zealand thyme, mānuka, kānuka, and clover honeys. Sugars, minerals, targeted phenolics, and bioactive indices were profiled alongside a functional panel (ferric reducing antioxidant power, FRAP; cupric ion reducing antioxidant capacity, CUPRAC; 1,1-diphenyl-2-picrylhydrazyl radical scavenging, DPPH; and anti-tyrosinase). Univariate analysis revealed a distinct functional gradient ($p \leq 0.004$), with thyme showing the highest mean activity across the four in vitro endpoints within this cohort. Beyond univariate comparison, data integration analysis for biomarker discovery using latent components (DIABLO), supervised by categorical honey type, and sparse partial least squares regression (sPLS-REG), using the continuous assay panel as the response, identified a bioactivity-associated signature spanning multiple chemical domains. The high-bioactivity axis co-varied with vitamin C, syringic acid, phosphorus, and sucrose; these associations do not establish biochemical synergy or soil causation. Botanical adjustment weakened or reversed several pooled associations; vitamin C–CUPRAC depended on the inference method and within-thyme support, and no pair passed within-type permutation BH correction. Lumichrome showed a kānuka-associated pattern within the present cohort, consistent with previous reports, but its specificity requires confirmation in larger, independently sourced cohorts. The contribution is the within-cohort integration of complementary compositional domains with multiple functional endpoints. The findings are hypothesis-generating and require external validation.

Keywords: honey; multiblock data integration; antioxidant capacity; thyme honey; authentication; lumichrome

Academic Editors: Ivana Tlak Gajger and Josipa Vlainić

Received: 1 September 2026
Revised: 18 October 2026
Accepted: 23 October 2026
Published: 1 November 2026

Copyright: © 2026 by the authors. Licensee MDPI, Basel, Switzerland. This article is an open access article distributed under the terms and conditions of the Creative Commons Attribution (CC BY) license.

1. Introduction

Honey is a naturally derived functional food. It is valued for its diverse bioactivities, including notable antioxidant and enzyme-inhibitory properties [1]. While phenolic acids and flavonoids are frequently cited as the primary drivers of these effects, the total

bioactive capacity is the product of a complex chemical matrix. This functional profile is supported by a suite of non-phenolic constituents, including ascorbic acid, endogenous enzymes (e.g., catalase, glucose oxidase), organic acids, and Maillard reaction products, as well as minerals that influence the overall redox environment. Consequently, honey bioactivity is not a static trait, but a variable phenotype determined by botanical origin and post-harvest factors such as processing and storage [2–6].

Botanical origin is the primary determinant of honey's phytochemical profile, driving distinct variations in colour and functional potential. Generally, darker honeys (e.g., certain *Leptospermum* spp.) contain higher levels of phenolic pigments and tend to demonstrate stronger antioxidant capacity than lighter honeys [7]. In the New Zealand context, mānuka (*Leptospermum scoparium*) honey is the most prominent example, renowned for its unique phytochemicals (e.g., methylglyoxal) and potent bioactivities. However, other regionally significant monoflorals such as kānuka (*Kunzea ericoides*), thyme (*Thymus vulgaris*), and clover (*Trifolium* spp.) possess their own characteristic chemical markers and health-promoting properties [8–10], warranting comparative investigation.

To map the functional potential of these honeys, this study focuses on four complementary bioactivity endpoints: ferric reducing antioxidant power (FRAP), 1,1-diphenyl-2-picrylhydrazyl (DPPH) radical scavenging, cupric ion reducing antioxidant capacity (CUPRAC), and anti-tyrosinase activity. Antioxidant activity is multifaceted, with different in vitro assays responding selectively to the diverse redox-active components present in the matrix; accordingly, multiparametric testing provides a more robust assessment than any single assay [9,11]. Tyrosinase inhibition was additionally quantified because this enzyme is central to melanogenesis and enzymatic browning, and its activity is known to be modulated by phenolic-rich matrices and vitamin C [12].

Prior comparative studies establish a distinct functional profile among New Zealand monofloral honeys. Thyme honey consistently ranks among high-performance varieties, often exceeding mānuka in reducing power and radical-scavenging activity. This elevated profile is supported by independent studies reporting strong antioxidant behaviour and measurable tyrosinase inhibition for *Thymus* honeys in different regions [9,13–15]. Conversely, clover honey serves as a lower-activity benchmark, characterised by lighter pigmentation and modest antioxidant responses [16–18]. Mānuka and kānuka honeys typically occupy an intermediate position for broad antioxidant assays [9]. While mānuka is renowned for specific antibacterial properties, its general antioxidant performance often varies depending on the specific redox mechanisms targeted [19,20]. Regarding enzyme inhibition, higher anti-tyrosinase activity is generally associated with darker, phenolic-rich honeys [12,21], linking this property to the broader bioactive capacity of the matrix [22–24].

Beyond phenolic composition, honey bioactivities frequently co-vary with broader compositional domains that are also strongly dependent on floral source. Mineral-related parameters have repeatedly been linked with honey antioxidant behaviour, supporting the idea that minerals and pigments co-vary with redox readouts rather than acting as isolated drivers [25,26]. Furthermore, the high concentration of reducing sugars in the matrix can complicate these measurements. Because assays such as FRAP rely on electron transfer, the sugars themselves can contribute to the reaction signal, potentially inflating the apparent antioxidant capacity independent of the phenolic content [4]. While recent profiling of New Zealand monoflorals has measured these parameters alongside bioactive indices, these relationships have rarely been modelled as an explicit cross-block association structure spanning sugars, minerals, and targeted small molecules [9,27]. Collectively, these findings suggest that honey bioactivities arise from coordinated variation across multiple chemical compartments rather than a single explanatory variable.

Recent honey characterisation has combined elemental metabolomics with chemometrics and volatile fingerprinting with interpretable machine learning for botanical or geographical authentication [28,29]. Our earlier volatile fingerprinting study [29] used the same physical honey cohort for botanical classification; the present work integrates non-volatile composition with four bioactivity endpoints to examine composition–function co-variation.

Most studies assess one chemical domain at a time, and when multivariate data fusion is employed, it is largely restricted to authentication tasks rather than explicitly mapping the composition–bioactivity association structure. To address this gap, this study uses DIABLO supervised by honey type to summarise coordinated variation across composition and bioactivity blocks. Furthermore, sparse PLS regression (sPLS-REG) is used to provide an interpretable, feature-selected view of the resulting multiblock signature [30,31]. By coupling these techniques, the research aims to move beyond single-domain profiling and provide a stability-guided map of the multi-constituent signatures associated with bioactivity in New Zealand monofloral honeys.

The contribution lies in integrating sugars, minerals, targeted phenolics, and bioactive indices with FRAP, CUPRAC, DPPH, and anti-tyrosinase in the same sample cohort using complementary multiblock association approaches. The previously reported antioxidant ranking of thyme, its vitamin C enrichment, and the association of lumichrome with kānuka are not presented as first discoveries; the focus is on composition–bioactivity co-variation rather than authentication performance.

2. Materials and Methods

2.1. Honey Samples

A total of 22 New Zealand monofloral honey samples were included in this study: thyme (n = 13), mānuka (n = 3), kānuka (n = 3), and clover (n = 3) (Supplementary Table S1). Both raw and commercial honeys were intentionally included to capture natural variability relevant to consumer products. Raw samples were sourced directly from producers with full traceability, while commercial samples were purchased from certified suppliers. Full metadata (floral designation, processing status, collection year, and geographic origin) are provided in Supplementary Table S1. The sample distribution was weighted towards thyme honey, reflecting prior evidence of high antioxidant activity in this honey by George, Gannabathula, Lakshitha, Liu, Kantono and Hamid [9], with mānuka, kānuka, and clover included as established benchmarks for comparative bioactivity grading.

2.2. Chemicals and Reagents

All chemicals and reagents were of analytical grade or higher. Trolox (6-hydroxy-2,5,7,8-tetramethylchroman-2-carboxylic acid), 2,4,6-tris(2-pyridyl)-s-triazine (TPTZ), 2,2-diphenyl-1-picrylhydrazyl (DPPH), neocuproine, L-3,4-dihydroxyphenylalanine (L-DOPA), mushroom tyrosinase, and kojic acid were purchased from Sigma Aldrich (Merck, Darmstadt, Germany). Iron(III) chloride ($FeCl_3$), copper(II) chloride ($CuCl_2$), hydrochloric acid (HCl), sodium acetate/acetic acid, ammonium acetate, and phosphate buffer reagents were of analytical grade or higher. Absolute ethanol and methanol were purchased from Thermo Fisher Scientific (Waltham, MA, USA) and were of HPLC or analytical grade. All solutions were prepared using distilled or deionised water.

2.3. Antioxidant Assays (FRAP, CUPRAC, and DPPH)

Antioxidant capacity was assessed using freshly prepared honey solutions (0.05 g/mL for FRAP/CUPRAC; 0.20 g/mL for DPPH) in distilled water. All assays were calibrated against Trolox standards, and results were expressed as mg Trolox Equivalents

(TE) per 100 g of honey. Assay conditions were based on established FRAP, CUPRAC, and DPPH protocols, with minor modifications aligned with recent applications to New Zealand monofloral honeys [9].

2.3.1. Ferric Reducing Antioxidant Power (FRAP)

The assay followed established protocols using a working reagent of acetate buffer (300 mM, pH 3.6), TPTZ (10 mM in 40 mM HCl), and $FeCl_3$ (20 mM) in a 10:1:1 ratio. Samples (100 µL) were incubated with the reagent (2.0 mL) at 37 °C for 4 min; then the absorbance was measured at 593 nm.

2.3.2. Cupric Ion Reducing Antioxidant Capacity (CUPRAC)

Reduction of the copper(II)-neocuproine complex was measured at 450 nm. The reaction mixture comprised equal volumes (1 mL) of $CuCl_2$ (10 mM), neocuproine (7.5 mM), and ammonium acetate buffer (1 M, pH 7.0), plus the sample (1 mL) and water (0.1 mL). Absorbance was recorded after 30 min of incubation to ensure reaction completion.

2.3.3. DPPH Radical Scavenging Capacity

The DPPH assay was performed according to the established DPPH radical-scavenging principle (absorbance monitored at 517 nm), with minor modifications outlined below. Honey solutions were prepared at 0.20 g/mL in distilled water. Buffered ethanol was prepared by mixing 100 mL of 0.1 M acetate buffer with 150 mL of absolute ethanol (total 250 mL). A 0.2 mM DPPH solution was prepared by dissolving 0.0079 g DPPH in 100 mL of methanol. Radical scavenging activity was determined by mixing honey solution (0.5 mL) with methanolic DPPH (0.2 mM, 2.0 mL) and methanol (4.0 mL). The control contained buffered ethanol (0.50 mL), DPPH solution (2.0 mL) and methanol (4.0 mL); the reference blank contained buffered ethanol (0.50 mL) and methanol (6.0 mL). Mixtures were incubated in the dark for 30 min, and absorbance was monitored at 517 nm. Trolox standards were used to generate a calibration curve, and results were expressed as mg TE/100 g honey.

DPPH inhibition (%) was calculated as:

$$Inhibition\ of\ DPPH(\%) = \left(\frac{Ac\ -\ As}{Ac}\right) \times 100$$

Ac: absorbance of control.

As: absorbance of the sample.

2.4. Anti-Tyrosinase Activity

Tyrosinase inhibition was measured using mushroom tyrosinase with L-DOPA as the substrate, based on the procedure of Di Petrillo, Santos-Buelga, Era, González-Paramás, Tuberoso, Medda, Pintus and Fais [21], with slight modifications for honey matrices and instrument settings. Reactions were prepared in 0.02 M phosphate buffer (pH 6.8) containing honey (6.25–50%, *w*/*v*) or buffer (controls) and L-DOPA (3.2 mM). The reaction was initiated by adding mushroom tyrosinase (200 U/mL stock; added to the reaction mix), and tyrosinase activity was monitored by measuring dopachrome formation at 492 nm using an Infinite 200 PRO M Plex multimode microplate reader (Tecan, Männedorf, Switzerland). Kojic acid was included as a positive control inhibitor. To correct for honey colour/background, matched sample blanks (honey + reagents without enzyme) were included for each concentration. Inhibition curves were summarised by the fitted half-response concentration (IC_{50}) from the selected nonlinear dose-response model in GraphPad Prism (version 8; GraphPad Software, San Diego, CA, USA). Kojic acid equivalents (KAE) were calculated from the blank-corrected IC_{50} values as a relative potency

ratio (IC_{50},kojic acid/IC_{50}, honey) after unit conversion, and reported as mg kojic acid equivalent inhibitory capacity per 100 g of honey.

2.5. Data Analysis

Statistical analyses were performed at the biological-sample level (n = 22) using Python (version 3.12.14) for univariate analyses and R (version 4.4.0) with the mixOmics package (version 6.30.0) for multivariate analyses. Technical assay triplicates were repeated analytical measurements of each honey and were averaged to obtain one observation per biological sample; they did not increase the biological sample size.

2.5.1. Data Pre-Processing and Endpoint Definitions

Bioactivity endpoints comprised FRAP, DPPH, CUPRAC, and anti-tyrosinase activity. All four endpoints were positive and complete at the biological-sample level in the data used for Table 1; no non-detect or non-positive substitution or imputation was applied to these endpoints.

Bioactivity endpoints were analysed on their original scale for reporting.

Table 1. Bioactivity of New Zealand monofloral honeys (thyme, mānuka, kānuka, and clover) measured by FRAP, DPPH, CUPRAC, and anti-tyrosinase assays.

Honey Type	FRAP (mg TE)/100 g Honey	DPPH (mg TE)/100 g Honey	CUPRAC (mg TE)/100 g Honey	Anti-Tyrosinase Activity (mg KAE)/100 g Honey
Thyme	129.51 ± 19.78 ^{a} (99.14–171.32)	89.42 ± 29.39 ^{a} (50.63–137.33)	88.47 ± 11.60 ^{a} (75.04–108.64)	17.13 ± 4.00 ^{a} (12.86–25.70)
Mānuka	54.06 ± 9.02 ^{b} (44.66–62.65)	28.30 ± 7.42 ^{b} (20.82–35.67)	53.05 ± 7.30 ^{b} (44.82–58.75)	10.30 ± 1.35 ^{b} (9.05–11.73)
Kānuka	59.66 ± 15.45 ^{b} (42.59–72.67)	23.11 ± 1.85 ^{b} (21.33–25.02)	64.15 ± 18.22 ^{ab} (44.82–81.01)	8.76 ± 0.59 ^{b} (8.08–9.13)
Clover	31.50 ± 15.18 ^{b} (14.14–42.26)	14.90 ± 7.00 ^{b} (7.68–21.67)	29.25 ± 11.52 ^{b} (16.33–38.43)	6.36 ± 0.82 ^{b} (5.42–6.97)
Omnibus Welch F	37.47	18.81	22.40	23.45
Omnibus p	<0.001	0.003	0.004	0.001

Values are mean ± SD with min–max in parentheses; FRAP, DPPH, and CUPRAC are expressed as mg Trolox equivalents (TE)/100 g honey. Anti-tyrosinase activity is reported as mg kojic acid equivalents (KAE)/100 g honey derived from IC_{50}-based relative potency. Different superscript letters within a column indicate significant differences (Welch ANOVA with Games–Howell post hoc, $p < 0.05$); omnibus Welch F and p values are shown.

2.5.2. Univariate Comparisons Across Honey Types

Honey-type differences in the four bioactivity assays were first assessed using Welch's one-way ANOVA, which is robust to unequal variances and suitable for the intentionally unbalanced design. Where the omnibus test indicated a honey-type effect, Games–Howell post hoc comparisons were used for pairwise testing. Results were summarised as mean ± SD for each honey type, and compact letter displays were used to indicate statistically homogeneous groups. Where multiple endpoints were assessed simultaneously, Benjamini–Hochberg FDR adjustment was applied to control for multiplicity.

2.5.3. Multiblock Integration (DIABLO)

To map co-variation between composition and bioactivity, we used DIABLO (mixOmics::block.splsda()) with categorical honey type as Y. Five matched X blocks contained

sugars (6 variables), minerals (9), targeted phenolics (15), bioactive indices [total phenolic content (TPC), total flavonoid content (TFC), vitamin C; 3], and bioactivity assays (FRAP, DPPH, CUPRAC, anti-tyrosinase; 4). Two components were fitted, with keepX equal to the number of variables in each block on both components; no sparsity tuning was performed. The supplied design matrix had off-diagonal entries of 0.1 and a zero diagonal. Variables were mean-centred and scaled to unit variance using scale(); no additional block-size normalisation was coded. The pre-processing removed non-varying or entirely non-finite columns, with named force-keep exceptions, and replaced non-finite scaled entries with zero; no separate near-zero-variance filter was specified. The script set seed 1. Circos plots summarised latent-component similarities among variables at cut-offs of $|r| \geq 0.80$ and $|r| \geq 0.60$. Although the fit was supervised by honey type, it was used here for exploratory association mapping; classification performance was not validated.

2.5.4. Multiblock sPLS Regression

Sugars, minerals, targeted phenolics, and bioactive constituents (total phenolic content, TPC; total flavonoid content, TFC; and ascorbic acid) were quantified for the same 22 honey samples using established protocols (Supplementary Methods S1–S4). Compositional summaries are reported in Supplementary Tables S3–S6.

Sparse partial least squares regression (mixOmics::block.spls()) used four compositional X blocks and the continuous four-assay Y matrix. The saved fit used indY = 5, two components per block, regression mode, the horst scheme, and scale = TRUE. The supplied X-block design had off-diagonal values of 0.1; the saved expanded design linked each X block to Y with weight 1. Final keepX values on each component were 6 for sugars, 9 for minerals, 3 for bioactive constituents, and 10 for phenolics; all four Y variables were retained. Stability was assessed using 200 stratified subsamples without replacement, nominal training fraction 0.80, a minimum of two honeys per type, and seed 1. This selected 10 of 13 thyme honeys and two of three from each other type per subsample. Input scaling preceded subsampling; it was not a validation pipeline. One block's keepX was varied at a time, while other blocks retained up to 10 variables per component. Selection frequency was the percentage of the 200 subsamples with a non-zero loading on either component. Signed combined loading magnitudes, $\sqrt{(l_1^2 + l_2^2)}$, were oriented using Spearman correlation between each feature and the mean standardised assay signal; resampled paths averaged these magnitudes only when a feature was selected. This assesses internal sensitivity of the present dataset and does not provide independent external validation or compensate for the small minority groups. Selected features were summarised by loadings, selection frequencies, and raw Spearman correlations with individual assays. All multivariate plots were exported as high-resolution PNG and fully editable SVG. The multiblock models were used for interpretation rather than prediction; therefore, the fitted association structure and selected feature patterns are reported without cross-validated performance metrics.

2.5.5. Botanical-Origin-Adjusted Association Sensitivity Analyses

To assess botanical-origin confounding, four previously highlighted constituents (vitamin C, syringic acid, phosphorus, and sucrose) were each paired with FRAP, CUPRAC, DPPH, and anti-tyrosinase, giving 16 separate follow-up comparisons (Table S7). Each used the 22 honey-level means and the retained original model-input values, without reclassifying recorded zeros. Pooled Pearson correlations were compared with partial correlations obtained by residualising X and Y on categorical honey type. Separate models Y ~ X + C(type) included four botanical levels, one common constituent slope, and 17 residual degrees of freedom. Recorded-unit slopes, pointwise HC3 95% confidence intervals and two-sided *p*-values used a Student-t reference. Benjamini–Hochberg q-values were

calculated over these 16 *p*-values. A separate 16-test correction applied to 9999 within-type response permutations using the absolute HC3-studentised slope statistic, seed 20261014, and $p = (\text{extreme} + 1)/10{,}000$. With fixed type effects, this shuffle is equivalent to permuting type-null residuals within type and restoring group means; it assumes within-type null exchangeability. Within-thyme Pearson/Fisher 95% intervals and Spearman correlations and leave-one-honey-out fits assessed sensitivity. Reported estimates are summarised in Table S7.

As a secondary global analysis, partial redundancy analysis related the four endpoints jointly to the four constituents after conditioning on honey type (Table S8). Type-residualised X and Y columns were scaled to unit sample standard deviation. The within-type R^2 used residual response variation as its denominator; its degrees-of-freedom adjustment was $1 - (1 - R^2) \times 18/14$. The global pseudo-F test used 9999 joint-response residual-row permutations restricted within type, preserving endpoint dependence; all 22 sample deletions were assessed separately. Calculations were independently reproduced in Python and R. These are exploratory, post-selection analyses of the same discovery cohort: correction across 16 comparisons does not account for earlier feature selection, and sensitivity analysis is not external validation. Table S8 summarises the full-model and deletion sensitivity results.

3. Results and Discussion

3.1. Antioxidant and Anti-Tyrosinase Activity Across Honey Types

Honey type had a significant effect on all bioactivity endpoints under the robust Welch ANOVA framework (FRAP $p < 0.001$; DPPH $p = 0.003$; CUPRAC $p = 0.004$; anti-tyrosinase $p = 0.001$; Table 1), revealing a consistent botanical gradient: thyme > mānuka/kānuka > clover. Thyme honey exhibited a 'broad-spectrum' efficacy, ranking highest across FRAP, DPPH, and anti-tyrosinase assays. While CUPRAC also showed the highest mean for thyme, kānuka occupied an intermediate position, with partial overlap (Table 1). Interpreting these assays together is important because they reflect different antioxidant chemistries: FRAP and CUPRAC primarily quantify electron-transfer reducing capacity, whereas DPPH reflects radical-scavenging behaviour [32,33]. Consequently, botanical differences can be directionally consistent without being identical across every endpoint, necessitating the use of multi-assay panels [11].

The elevated profile of the thyme samples is consistent with reports of substantial antioxidant activity in some *Thymus* honeys. This "thyme-high" direction replicates findings from recent New Zealand profiling [9], and several thyme honey studies that couple high antioxidant capacity with measurable tyrosinase inhibition [13,15,22,24]. Differences in redox-active composition offer a plausible basis for botanical variation, but the present study did not measure nectar chemistry, plant protective functions or their transfer into honey [15,22]. The observed thyme profile is consistent with botanical differences, but the present design does not separate floral origin from processing or other sample-history effects.

In contrast, mānuka and kānuka showed intermediate bioactivity profiles. Both were lower than thyme for FRAP, DPPH and anti-tyrosinase activity, whereas kānuka showed partial overlap with thyme for CUPRAC (Table 1). This highlights that "bioactivity" is mechanism-specific: the non-peroxide antibacterial factors (e.g., methylglyoxal) characteristic of *Leptospermum* do not necessarily translate to superior electron-transfer reducing power (FRAP/CUPRAC) compared to the vitamin-and-phenolic-rich Lamiaceae matrix. This interpretation is supported by the broader literature where mānuka's antioxidant performance is often moderate and context-dependent [19,20]. While mānuka has been reported as a potent tyrosinase inhibitor in other panels, kānuka inhibition remains less

documented, though the intermediate levels observed here contribute to its growing bioactive profile [23,24].

Clover honey exhibited the lowest mean overall bioactivity profile in our cohort (Table 1), showing the weakest response across all four assays. This "clover-lower" status is consistent with the lighter pigmentation and modest phenolic indices typical of *Trifolium* honeys [16]. Anti-tyrosinase activity for clover honeys remains poorly documented, and the lower inhibition is consistent with broader reports that lighter, lower-phenolic honeys tend to show weaker bioactivities like tyrosinase inhibition than darker, phenolic-richer monoflorals [12,17,21].

Vitamin C (ascorbic acid) is a strong electron donor that can contribute to measured antioxidant capacity across multiple in vitro assays, including FRAP/CUPRAC (reducing power) and DPPH (radical-scavenging), and it can also suppress tyrosinase-mediated browning by reducing o-quinones back to their corresponding catechols [4,9,12]. Univariate analysis confirmed that vitamin C levels were significantly higher in thyme honey (Supplementary Table S6), identifying it as a distinguishing compositional feature of thyme in this cohort, while its contribution to each endpoint requires experimental confirmation [9]. These contrasts provide a necessary foundation for the multiblock correlation mapping (DIABLO/sPLS-REG) that follows, which aims to interpret how coordinated sugar, mineral, and phenolic signatures co-vary with bioactivity.

Naturally sweet matrices provide useful context for these in vitro endpoints. Carob syrup extracts showed radical-scavenging and ferric-reducing activity, with extraction and simulated digestion influencing the readouts [34]. *Ziziphus lotus* fruit fractions likewise showed DPPH and reducing activity, although the tested material was an ethyl-acetate fraction of dried fruit, not the consumed fruit itself [35]. These studies place the present honeys within a broader range of plant-derived sweet matrices with measurable assay activity. They do not support numerical superiority: carob FRAP was reported in $FeSO_4$ equivalents, and the fruit study used extract $IC_{50}/A_{0.5}$ values and a ferricyanide reducing procedure at 700 nm rather than the TPTZ-based FRAP procedure used here. Extraction basis, assay chemistry and calibration therefore preclude direct ranking against our mg Trolox equivalents per 100 g honey. A Moroccan honey-extract study offers additional botanical context, but its DPPH IC_{50} and ferricyanide-based reducing assay are also not directly interchangeable with our protocols [36]. Qualitative comparison is therefore appropriate; these measurements do not establish clinical antioxidant benefits.

3.2. Multiblock Integrative Modelling

Building on the univariate results, we next apply multiblock integrative modelling to characterise how coordinated variation across sugars, minerals, targeted phenolics, and bioactive constituent metrics aligns with the measured bioactivities. This analysis is correlation-based and used to interpret the cross-block structure of honey bioactivity rather than inferring linear causality.

3.2.1. DIABLO Multiblock Integration and Circos Association Networks

To move beyond single-domain interpretation, DIABLO (block.splsda), supervised by categorical honey type, was applied to integrate the sugars, minerals, targeted phenolics, and "bioactive constituent" indices (TPC, TFC, vitamin C) with the bioactivity assays (FRAP, CUPRAC, DPPH, anti-tyrosinase). The strongest cross-block associations were visualised as a circos network (Comp 1–2; $|r| \geq 0.8$). DIABLO is used here as an association-mapping framework: links represent strong latent-component similarities across the same samples, reflecting the fact that floral source shifts multiple compositional domains simultaneously [30]. Thus, observed correlations capture coordinated "honey-type"

profiles rather than the action of single constituents in isolation. Full compositional results are reported in Supplementary Tables S3–S6.

The saved similarity table contained two strong within-bioactivity pairings at $|r| \geq 0.8$ (within-block chords were suppressed in Figure 1): FRAP and CUPRAC clustered tightly, consistent with both assays largely reflecting electron-transfer reducing capacity under different reagent systems, and DPPH and anti-tyrosinase co-varied, supporting a coupled "radical-scavenging/enzyme-inhibitory" axis. Importantly, this co-variation does not imply a single driver; rather, it summarises coordinated assay responses in the present cohort [26,37].

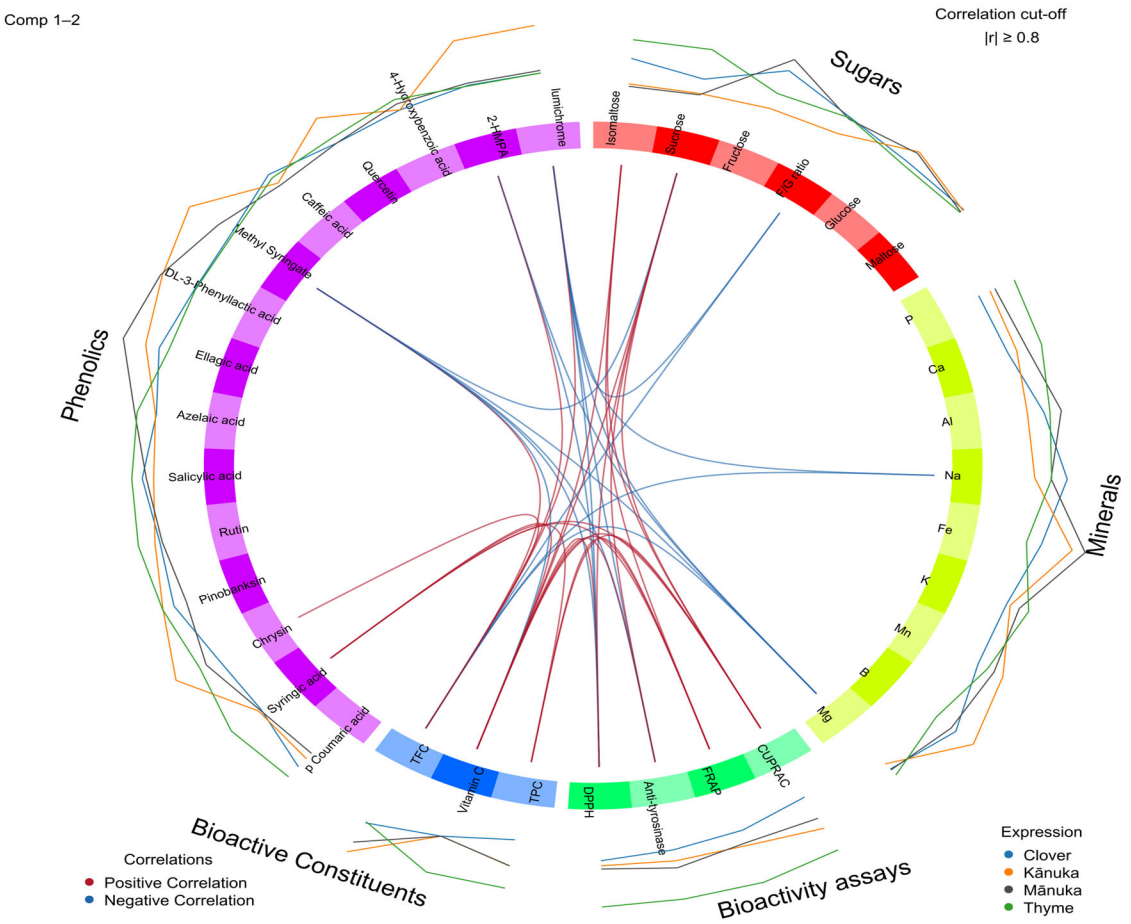


Figure 1. DIABLO circos association network linking composition blocks to bioactivity endpoints in New Zealand monofloral honeys. Circos plot summarising the strongest cross-block associations (DIABLO Comp 1–2) between sugars, minerals, targeted phenolics, and bioactive constituent indices (TPC, TFC, vitamin C) and the bioactivity assays (FRAP, CUPRAC, DPPH, anti-tyrosinase). Chords indicate latent-component similarities returned by circosPlot among variables retained at a stringent threshold ($|r| \geq 0.8$); red chords denote positive correlations, and blue chords denote negative correlations. Coloured traces outside the circle show the relative expression patterns for each selected variable across honey types (thyme, mānuka, kānuka, clover). The outer traces identify thyme (green), mānuka (grey/black), kānuka (orange), and clover (blue). Sector colours identify sugars (red), minerals (yellow-green), bioactivity assays (green), bioactive constituent indices (blue), and phenolics (purple). The phenolic abbreviation 2-HMPA denotes 2-hydroxy-3-(4-methoxyphenyl)propanoic acid.

The most prominent cross-block links into the bioactivity assays were concentrated in the bioactive constituent indices, especially vitamin C and TPC. Vitamin C showed strong positive associations with DPPH, CUPRAC, FRAP, and anti-tyrosinase at $|r| \geq 0.8$, coherent with ascorbic acid acting as a potent electron donor and an anti-browning agent [12]. In parallel, TPC showed strong positive links with CUPRAC and FRAP, aligning with the role of phenolic richness as a broad indicator of honey's reducing capacity and antioxidant potential [38–40]. Crucially, the higher vitamin C and TPC values in the same samples are consistent with a coordinated compositional profile in the present honey cohort, rather than an isolated pairwise effect [9].

At the level of individual phenolics, the network showed distinct interaction patterns. The syringic acid signal showed strong positive associations with CUPRAC and FRAP, consistent with a phenolic-acid-rich axis that tracks reducing power. In contrast, markers such as methyl syringate and lumichrome displayed negative associations with the bioactivity block. These negative links represent pattern-level contrasts (i.e., markers of the lower-activity mānuka/kānuka profiles) rather than biochemical suppression. However, the lumichrome-associated separation of kānuka samples is chemically significant. Lumichrome showed a kānuka-associated pattern within the present cohort, consistent with previous reports [41,42]. Its specificity requires confirmation in larger, independently sourced cohorts; the present dataset does not validate genus specificity or authentication performance [43].

Within the sugar block, only sucrose and isomaltose exceeded the stringent threshold for direct linkage to bioactivity. These associations are best interpreted as matrix co-variation, where floral source and processing shift carbohydrate profiles alongside redox-active constituents [44,45]. Similarly, while mineral content is known to influence honey conductivity and redox behaviour, no single mineral met the strict $|r| \geq 0.80$ threshold for direct linkage in this network. This suggests that mineral co-variation may be summarised more broadly by the latent-variable approach of sPLS regression (Section 3.2.2), without establishing synergy or a mineral mechanism.

Overall, the DIABLO circos network provides a compact summary of the co-variation between composition and bioactivity. Under the stringent main-text threshold ($|r| \geq 0.80$), the analysis supports the interpretation that the bioactivity-aligned structure is multi-constituent, bridging phenolic richness and vitamin content with matrix-specific sugar profiles. An extended circos network at a lower threshold ($|r| \geq 0.60$) is provided in Supplementary Figure S1 alongside the main-text strict network ($|r| \geq 0.80$). Across both networks, the purpose is interpretive: to summarise sample-level co-variation across honey types without implying biochemical causality.

3.2.2. Multiblock sPLS Regression of Compositional Blocks Against Bioactivity Assays

Following the DIABLO circos association map, multiblock sparse PLS regression (sPLS-REG; mixOmics) was employed as a complementary, multivariate way to summarise which variables contribute most strongly to the shared composition–bioactivity covariance. Unlike the circos network, which visualises high-threshold latent-component similarities, sPLS-REG provides a component-based summary that accommodates collinearity and extracts a sparse set of features whose weighted combinations best track the multivariate bioactivity signal [30,31]. This is treated as an interpretive association model: floral origin shifts multiple compositional domains simultaneously, so multivariate loadings are interpreted as signatures of coordinated honey-type profiles rather than single-compound "drivers" in isolation.

Two complementary visual summaries are shown. First, the combined loadings bars (Comp 1–2; Figure 2A–D) rank variables by magnitude, $\sqrt{(l_1^2 + l_2^2)}$, and direction relative to the bioactivity signal. Second, the stability paths (Figure 3A–D) track signed combined

loading magnitudes across 200 stratified subsamples (nominal train = 0.8), assessing internal sensitivity to sample and sparsity perturbations.

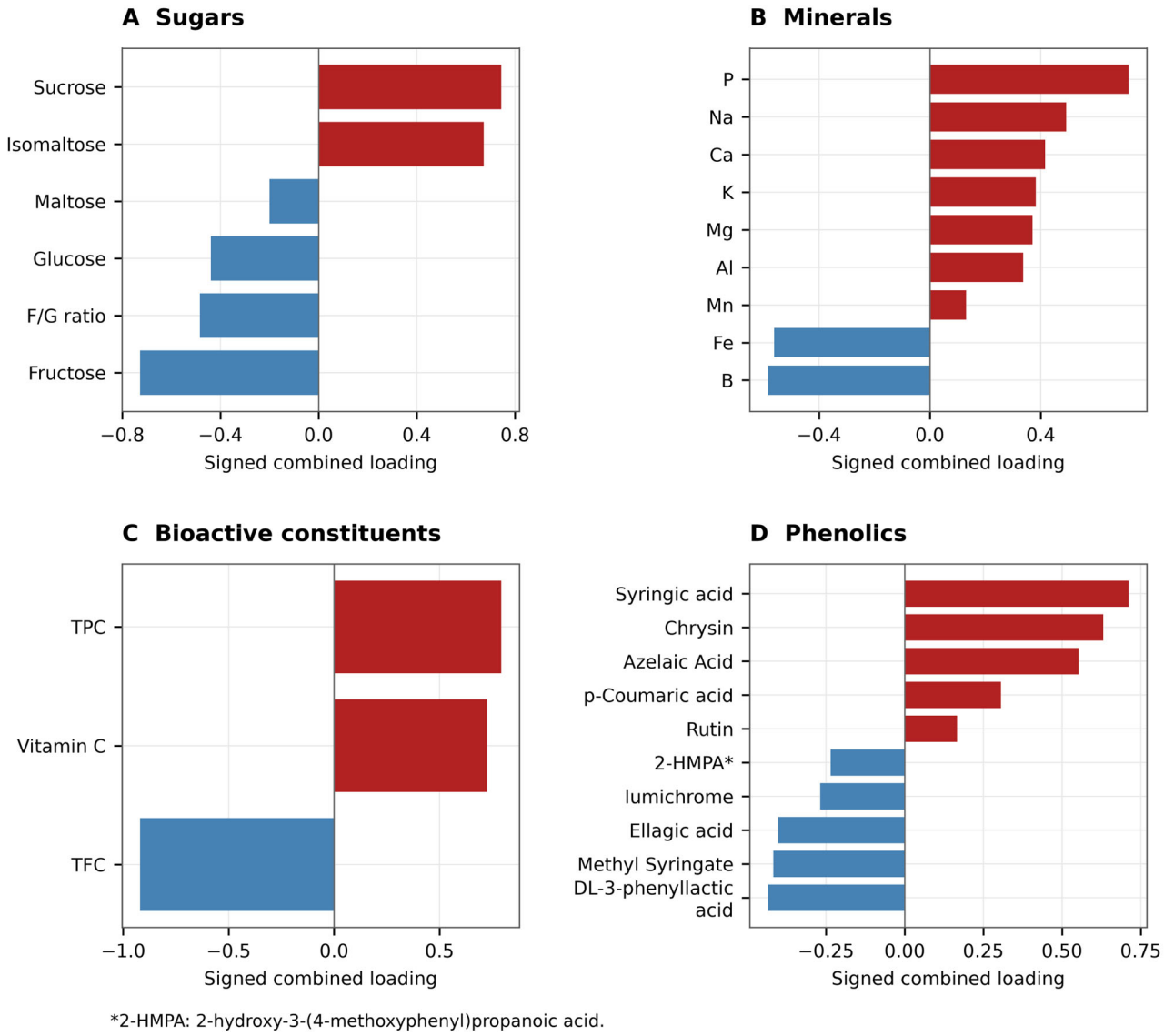
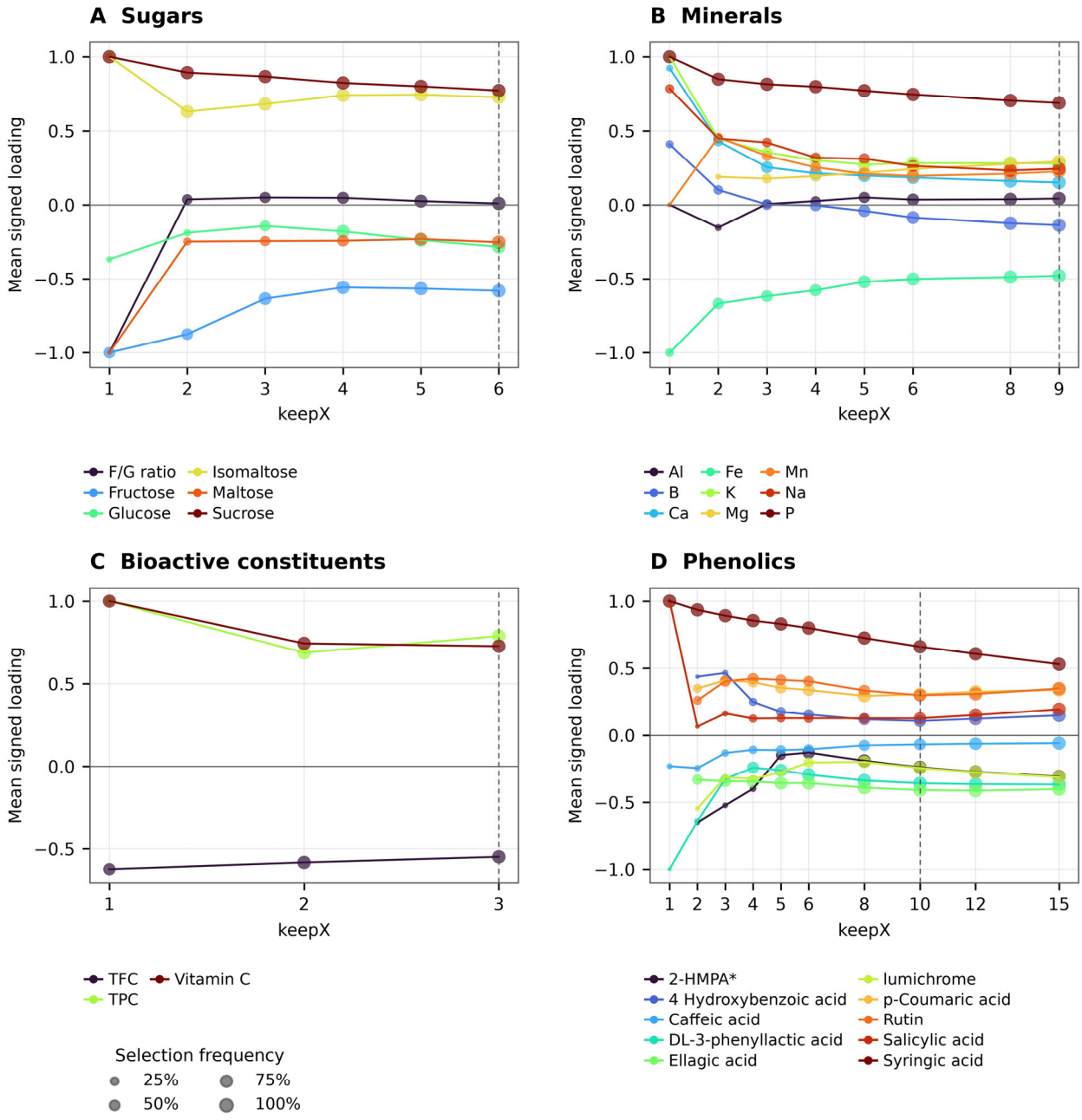


Figure 2. Multiblock sPLS regression (sPLS-REG) combined loadings across compositional blocks for the joint bioactivity signal (Comp 1–2). Panels show (**A**) sugars, (**B**) minerals, (**C**) bioactive constituents (TPC, TFC, vitamin C), and (**D**) targeted phenolics. Bars represent the signed combined loading magnitude for each selected variable within each block, ranked by $\sqrt{(l_1^2 + l_2^2)}$. The sign is anchored by Spearman correlation of each feature with the mean standardised assay signal (*Y* block: FRAP, CUPRAC, DPPH, and anti-tyrosinase), such that positive bars indicate co-variation with higher overall bioactivity and negative bars indicate co-variation in the opposite direction. The plot is interpreted as descriptive association structure (co-variation), not mechanistic causality.

Across all blocks, the bioactive constituent indices (TPC and vitamin C) were among the most prominent positive features and the most stable in the resampling view (Figures 2C and 3C). Both measures remained positive across sparsity settings, indicating that their alignment with the multivariate assay response is an internally persistent pattern in this dataset. Notably, under maximal sparsity (keepX = 1), vitamin C displayed a higher selection frequency than TPC (Figure 3C). This stability reinforces the DIABLO findings, supporting ascorbic acid as a bioactivity-associated feature within this cohort. Biochemically, this is coherent: FRAP and CUPRAC quantify electron-transfer reducing capacity, and the

broad redox-active pools captured by vitamin C and TPC are expected to contribute to these readouts [38–40]. Meanwhile, vitamin C is a strong electron donor and is widely discussed in the context of redox cycling relevant to quinone reduction and browning-related chemistry, providing a coherent conceptual basis for parallel trends across antioxidant and anti-tyrosinase endpoints when a sample set spans contrasting "high-activity" versus "low-activity" honey matrices [12].



*2-HMPA: 2-hydroxy-3-(4-methoxyphenyl)propanoic acid.

Figure 3. Multiblock sPLS regression (sPLS-REG) signed loading paths versus sparsity (keepX) showing internal sensitivity of blockwise associations with bioactivity. Panels show (**A**) sugars, (**B**) minerals, (**C**) bioactive constituent indices (TPC, TFC, vitamin C), and (**D**) targeted phenolics. For each block, lines track the mean signed combined loading magnitude, $\sqrt{(l_1^2 + l_2^2)}$, conditional on selection across repeated subsamples while varying keepX (number of variables retained). Point size indicates selection frequency (stability, %), and the vertical dashed line marks the chosen keepX

used for the final reported signature. Signs are anchored within each subsample by Spearman correlation between each feature and the mean standardised bioactivity signal, such that positive values correspond to variables that increase with higher assay response and negative values indicate the opposite direction. The paths are used to assess the stability of the descriptive association pattern under tuning variation, not predictive performance.

Within the targeted phenolics block, the signature was dominated by syringic acid (the largest positive bar), followed by chrysin and azelaic acid, with *p*-coumaric acid and rutin also contributing positively (Figure 2D). The internal stability analysis shows persistence of this positive loading across keepX settings (Figure 3D), supporting the interpretation that a specific phenolic-acid/phenolic enrichment axis is consistently embedded within the integrated bioactivity co-variance. This aligns with the consensus that phenolic richness is a major contributor to honey's reducing capacity and radical-scavenging behaviour [38–40]. Conversely, markers such as methyl syringate and lumichrome loaded negatively. In sPLS-REG, this negativity represents profile contrast: these compounds characterise the alternative kānuka/mānuka phenotypes and thus oppose the latent component tracking the high-activity thyme signature.

The minerals block contributes a coherent multielement signature rather than a single dominant "driver" (Figure 2B). Phosphorus (P) showed the strongest positive loading and was the most stably retained element in the internal stability analysis (Figure 3B), accompanied by Na, Ca, K, Mg, Al, and Mn. Published studies relate multielement honey profiles to geographical context; this literature provides background rather than evidence of soil causation in the present samples [46,47]. No soil samples were analysed, so the phosphorus loading cannot establish soil-derived phosphorus, a regional geological mechanism, or geographical verification. Honey antioxidant and anti-tyrosinase behaviour is more commonly attributed to phenolic and other redox-active constituents, including ascorbic acid [48]. Here, phosphorus and the broader mineral profile co-vary with the bioactivity-aligned multivariate structure. These cohort-specific associations generate hypotheses for future studies that directly measure environmental factors and test constituent effects.

Although the sugar block is small, it displayed a distinct co-variation pattern: sucrose and isomaltose loaded positively, while fructose loaded negatively (Figures 2A and 3A). Sucrose was the most internally persistent sugar feature, maintaining a consistently positive trend across sparsity levels (Figure 3A). While sugars are not primary redox agents, this pattern highlights the importance of the matrix environment. The positive loading of sucrose suggests that the carbohydrate profile of the thyme honeys co-varies with the accumulation of redox-active constituents. This is consistent with the interpretation that "high bioactivity" is not an isolated trait but part of a specific honey matrix defined by both its organic (phenolic) and carbohydrate composition [44,45].

Taken together, Figures 2A–D and 3A–D show that the sPLS-REG model summarises coordinated associations between bioactivity and phenolic/vitamin, mineral, and sugar profiles. The consistency across resampling (Figure 3A–D) indicates internal persistence in the present dataset and does not provide external validation. The integration provides a hypothesis-generating account of composition–bioactivity co-variation without identifying soil inputs or causal constituent effects. The sPLS-REG stability paths (selection frequency across keepX based on 200 resamples) for each block are provided in Supplementary Figure S2, and the corresponding selected feature–assay association heatmap (raw Spearman *r*) is shown in Supplementary Figure S3.

3.2.3. Botanical-Origin Sensitivity and Functional Interpretation

The retained model-input analysis showed that botanical adjustment substantially changed several pooled associations (Table S7). Vitamin C–CUPRAC remained positive (pooled $r = 0.829$; partial $r = 0.598$; adjusted slope = 0.5785, HC3 95% CI 0.3466–0.8103, in recorded assay units per retained vitamin C unit). It was the only association with HC3 BH $q < 0.05$ ($p = 0.0000634$; $q = 0.001014$), whereas its restricted-permutation $p = 0.0040$ and $q = 0.0640$ did not pass the separate permutation FDR threshold. None of the 16 comparisons passed permutation BH $q < 0.05$. Vitamin C–FRAP remained positive but uncertain (partial $r = 0.515$; HC3 $p = 0.0807$; $q = 0.3228$), while its DPPH and anti-tyrosinase associations weakened to partial $r = -0.074$ and 0.134. Syringic acid–DPPH reversed direction (pooled $r = 0.638$; partial $r = -0.632$; HC3 $p = 0.0193$; $q = 0.1432$), and phosphorus–DPPH remained positive (partial $r = 0.602$; HC3 $p = 0.0269$; $q = 0.1432$); neither passed either FDR procedure. All sucrose associations were non-significant after adjustment, with negative FRAP/CUPRAC slopes and near-zero DPPH/anti-tyrosinase partial correlations. The remaining comparisons and their uncertainty are reported in full in Table S7. Attenuation after adjustment does not establish botanical origin as the sole explanation, because limited within-type variation and small groups reduce power.

Vitamin C–CUPRAC was also positive within thyme ($n = 13$; Pearson $r = 0.766$, Fisher 95% CI 0.372–0.926; Spearman $\varrho = 0.687$), and its adjusted slope remained positive across honey deletions (0.5147–0.6445). However, all nine non-thyme vitamin C entries were recorded zeros, so its within-type evidence came entirely from thyme, and it cannot establish a common relationship across botanical populations. Deletions changed the adjusted slope sign for vitamin C–DPPH (2/22), sucrose–DPPH (4/22), and sucrose–anti-tyrosinase (2/22). Secondary partial RDA accounted for 42.08% of in-sample within-type multivariate response variation (df-adjusted 25.53%; pseudo-$F_{4,14} = 2.543$; permutation $p = 0.0288$; Table S8), rather than 42.08% of total response variation. The global p ranged from 0.0061 to 0.1314 after sample deletion, reaching ≥0.05 in eight deletions. Thyme supplied 91.7% of standardised within-type predictor variation. These results qualify the pooled multiblock signature; they do not confirm causal constituent effects or independently replicated associations across honey types.

To maintain strict continuity with the primary multiblock models, all botanical-adjustment and sensitivity analyses were performed directly on the locked model-input matrix. Because non-thyme vitamin C values were recorded as below-detection zeros in this matrix, within-type variance for vitamin C is restricted to the thyme group, and the resulting cross-group slope estimates should be interpreted within the context of the archived model scale. Functional interpretation must distinguish assay chemistry from compositional association. Vitamin C is a plausible direct reducing contributor to FRAP and CUPRAC, while its DPPH response depends on reaction conditions; pure-compound experiments support these redox activities but do not quantify its contribution in honey [49,50]. Syringic acid has shown FRAP and DPPH activity as an isolated standard [50], but its negative adjusted DPPH association here is not evidence of antioxidant suppression. Direct syringic-acid contributions to CUPRAC or tyrosinase inhibition at the concentrations present were not established by this study. FRAP/CUPRAC reduction, DPPH scavenging, and the IC_{50}-derived kojic-acid-equivalent endpoint are distinct responses. The anti-tyrosinase readout does not identify which constituent inhibits the enzyme; mechanistic interpretation requires controls distinguishing enzyme inhibition from coupled redox reactions [12].

Elemental phosphorus and sucrose are therefore treated as indirect compositional markers, rather than demonstrated mediators of any of the four endpoints. Phosphorus speciation and direct constituent effects were not measured. Sugar-related viscosity or other matrix effects are possibilities requiring matched controls, not established explanations for the sucrose loadings. Similarly, Folin–Ciocalteu TPC is an operational reducing-

reactivity index that also responds to non-phenolic compounds, including ascorbate [51]; agreement with FRAP/CUPRAC need not reflect independent phenolic-specific effects. Standard-compound tests at measured concentrations, spiking/removal and controlled phenolic-fraction experiments with matrix, colour and tyrosinase-interferent controls, and larger balanced independently sampled botanical cohorts are needed to separate functional contributions from co-variation.

The study is an exploratory proof-of-principle analysis of 22 independent honeys: thyme (n = 13), mānuka (n = 3), kānuka (n = 3), and clover (n = 3). The small, unbalanced minority groups cannot establish population-level specificity or broad generalisability. Technical triplicates describe analytical repeatability, and internal resampling does not supply new biological observations or independent validation. Floral origin may be confounded with region, collection year, raw/commercial status, processing, and storage. Larger, balanced, independently sourced cohorts spanning these factors are required to test the associations and any proposed authentication or predictive application.

4. Conclusions

This study compared the antioxidant (FRAP, CUPRAC, DPPH) and anti-tyrosinase activities of four New Zealand monofloral honeys and used correlation-focused multiblock integration to interpret how these bioactivities co-vary within a multi-domain composition. Under a robust Welch/Games–Howell framework, honey type significantly affected each bioactivity endpoint, with thyme showing the highest mean activity across the four in vitro endpoints in this cohort; Games–Howell overlap for CUPRAC is retained in Table 1.

Building on this foundation, DIABLO supervised by categorical honey type and multiblock sPLS regression with the continuous assay response were applied as interpretive association models (not causal or predictive validation models) to map coordinated variation between sugars, minerals, targeted phenolics, and bioactive constituents (TPC, TFC, vitamin C). Across both multiblock views, the bioactivity-aligned structure was cross-domain and internally consistent, supporting a coordinated honey-matrix pattern within the present cohort. The associations of phosphorus, vitamin C, syringic acid, and sugar profiles reflect cross-domain co-variation, without establishing soil causation or biochemical synergy. Stability under sparsity and subsampling perturbations describes internal sensitivity rather than external validation. Lumichrome showed a kānuka-associated pattern consistent with previous reports; the three kānuka samples do not establish genus specificity or authentication performance. The contribution is the joint interpretation of multiple compositional domains against four functional endpoints in the same cohort. Larger, balanced, independently sourced cohorts spanning regions and production years are required before predictive, authentication, or regulatory use can be considered.

Botanical-type adjustment qualifies the pooled signature: the vitamin C–CUPRAC association depends on the inference procedure and within-thyme support, while the other constituent-specific comparisons do not pass FDR control; the exploratory global association is sensitive to sample deletion.

Supplementary Materials: The following supporting information can be downloaded at: https://www.mdpi.com/article/10.3390/antiox15111415/s1, Table S1: Summary of honey samples; Table S2: Sample-wise bioactivity values; Methods S1–S4: analytical methods for sugars, minerals, targeted phenolics, and bioactive constituents; Tables S3–S6: sugar, mineral, targeted phenolic, and bioactive constituent results; Figure S1: Extended DIABLO circos network ($|r| \geq 0.60$); Figure S2: sPLS-REG stability paths across sparsity settings; Figure S3: Spearman correlation heatmap between selected features and individual bioactivity assays. Tables S7: exploratory botanical-origin-adjusted constituent–bioactivity associations; S8: secondary partial-RDA sensitivity analysis, respectively.

https://doi.org/10.3390/antiox15111415

Author Contributions: Conceptualisation, R.L. and N.H.; methodology, R.L., N.H., K.K. and A.O.; software, K.K. and A.O.; formal analysis, R.L. and K.K.; investigation, R.L.; resources, N.H., T.T.L., A.O. and S.G.; data curation, R.L.; writing - original draft preparation, R.L.; writing - review and editing, N.H.; visualisation, R.L. and K.K.; supervision, N.H., T.T.L. and S.G.; project administration, N.H.; funding acquisition, N.H. All authors have read and agreed to the published version of the manuscript.

Funding:. This research received no external funding.

Institutional Review Board Statement: Not applicable. Informed Consent Statement: Not applicable.

Data Availability Statement: The original data presented in this study are included in the article and its Supplementary Materials (Tables S1–S8). Further inquiries can be directed to the corresponding author.

Conflicts of Interest: The authors declare no conflicts of interest.

References

1. Al Qahtani, H.W.S.; Yagi, S.; Yılmaz, M.A.; Cakır, O.; Tarhan, A.; Mustafa, A.A.; Zengin, G. Chemical profile, antioxidant and enzyme inhibition activities of natural Saudi Sidr and Talh honeys. *Chem. Biodivers.* **2022**, *19*, e202200227.
2. Cianciosi, D.; Forbes-Hernández, T.Y.; Afrin, S.; Gasparrini, M.; Reboredo-Rodriguez, P.; Manna, P.P.; Zhang, J.; Bravo Lamas, L.; Martínez Flórez, S.; Agudo Toyos, P. Phenolic compounds in honey and their associated health benefits: A review. *Molecules* **2018**, *23*, 2322.
3. Bogdanov, S.; Jurendic, T.; Sieber, R.; Gallmann, P. Honey for nutrition and health: A review. *J. Am. Coll. Nutr.* **2008**, *27*, 677–689.
4. Chua, L.S.; Rahaman, N.L.A.; Adnan, N.A.; Eddie Tan, T.T. Antioxidant activity of three honey samples in relation with their biochemical components. *J. Anal. Methods Chem.* **2013**, *2013*, 313798.
5. Da Silva, P.M.; Gauche, C.; Gonzaga, L.V.; Costa, A.C.O.; Fett, R. Honey: Chemical composition, stability and authenticity. *Food Chem.* **2016**, *196*, 309–323.
6. Alves, A.; Ramos, A.; Gonçalves, M.M.; Bernardo, M.; Mendes, B. Antioxidant activity, quality parameters and mineral content of Portuguese monofloral honeys. *J. Food Compos. Anal.* **2013**, *30*, 130–138.
7. Bratosin, E.D.; Tit, D.M.; Purza, A.L.; Pasca, M.B.; Bungau, G.S.; Marin, R.C.; Radu, A.F.; Gitea, D. Exploratory Analysis of Phenolic Profiles and Antioxidant Capacity in Selected Romanian Monofloral Honeys: Influence of Botanical Origin and Acquisition Source. *Antioxidants* **2025**, *14*, 1248.
8. Alvarez-Suarez, J.M.; Gasparrini, M.; Forbes-Hernández, T.Y.; Mazzoni, L.; Giampieri, F. The Composition and Biological Activity of Honey: A Focus on Manuka Honey. *Foods* **2014**, *3*, 420–432. https://doi.org/10.3390/foods3030420.
9. George, E.M.; Gannabathula, S.; Lakshitha, R.; Liu, Y.; Kantono, K.; Hamid, N. Antibacterial Properties, Arabinogalactan Proteins, and Bioactivities of New Zealand Honey. *Antioxidants* **2025**, *14*, 375.
10. León-Ruiz, V.; Vera, S.; González-Porto, A.V.; Andrés, M.P.S. Vitamin C and sugar levels as simple markers for discriminating Spanish honey sources. *J. Food Sci.* **2011**, *76*, C356–C361.
11. Gorjanović, S.Ž.; Alvarez-Suarez, J.M.; Novaković, M.M.; Pastor, F.T.; Pezo, L.; Battino, M.; Sužnjević, D.Ž. Comparative analysis of antioxidant activity of honey of different floral sources using recently developed polarographic and various spectrophotometric assays. *J. Food Compos. Anal.* **2013**, *30*, 13–18.
12. Zolghadri, S.; Bahrami, A.; Hassan Khan, M.T.; Munoz-Munoz, J.; Garcia-Molina, F.; Garcia-Canovas, F.; Saboury, A.A. A comprehensive review on tyrosinase inhibitors. *J. Enzym. Inhib. Med. Chem.* **2019**, *34*, 279–309.
13. Sánchez-Martín, V.; Morales, P.; González-Porto, A.V.; Iriondo-DeHond, A.; López-Parra, M.B.; Del Castillo, M.D.; Hospital, X.F.; Fernández, M.; Hierro, E.; Haza, A.I. Enhancement of the antioxidant capacity of thyme and chestnut honey by addition of bee products. *Foods* **2022**, *11*, 3118.
14. Fernández-Estellé, M.; Hernández-González, V.; Saurina, J.; Núñez, O.; Sentellas, S. Characterization and classification of Spanish honeydew and blossom honeys based on their antioxidant capacity. *Antioxidants* **2023**, *12*, 495.
15. León-Ruiz, V.; González-Porto, A.V.; Al-Habsi, N.; Vera, S.; San Andrés, M.P.; Jauregi, P. Antioxidant, antibacterial and ACE-inhibitory activity of four monofloral honeys in relation to their chemical composition. *Food Funct.* **2013**, *4*, 1617–1624.

16. Ciappini, M.C.; Stoppani, F.S. Determination of antioxidant capacity, flavonoids, and total phenolic content in eucalyptus and clover honeys. *J. Apic. Sci.* **2014**, *58*, 103.
17. Sultana, S.; Foster, K.; Bates, T.; Hossain, M.L.; Lim, L.Y.; Hammer, K.; Locher, C. Determination of Physicochemical Characteristics, Phytochemical Profile and Antioxidant Activity of Various Clover Honeys. *Chem. Biodivers.* **2024**, *21*, e202301880.
18. Can, Z.; Yildiz, O.; Sahin, H.; Turumtay, E.A.; Silici, S.; Kolayli, S. An investigation of Turkish honeys: Their physico-chemical properties, antioxidant capacities and phenolic profiles. *Food Chem.* **2015**, *180*, 133–141.
19. Morar, I.I.; Pop, R.M.; Peitzner, E.; Ranga, F.; Orăsan, M.S.; Cecan, A.D.; Chera, E.I.; Bonci, T.I.; Usatiuc, L.O.; Țicolea, M. Phytochemical composition and antioxidant activity of Manuka honey and Ohia Lehua honey. *Nutrients* **2025**, *17*, 276.
20. Pentoś, K.; Łuczycka, D.; Oszmiański, J.; Lachowicz, S.; Pasternak, G. Polish honey as a source of antioxidants–a comparison with Manuka honey. *J. Apic. Res.* **2020**, *59*, 939–945.
21. Di Petrillo, A.; Santos-Buelga, C.; Era, B.; González-Paramás, A.M.; Tuberoso, C.I.G.; Medda, R.; Pintus, F.; Fais, A. Sardinian honeys as sources of xanthine oxidase and tyrosinase inhibitors. *Food Sci. Biotechnol.* **2018**, *27*, 139–146.
22. Fratianni, F.; Ombra, M.N.; De Giulio, B.; d'Acierno, A.; Nazzaro, F. Lamiaceae honey: Polyphenol profile, vitamin C content, antioxidant and in vitro anti-inflammatory, cholinesterase and tyrosinase inhibitory activity. *Food Chem. Adv.* **2025**, *7*, 100996.
23. Jantakee, K.; Tragoolpua, Y. Activities of different types of Thai honey on pathogenic bacteria causing skin diseases, tyrosinase enzyme and generating free radicals. *Biol. Res.* **2015**, *48*, 4.
24. Stavropoulou, E.; Voidarou, C.; Rozos, G.; Vaou, N.; Bardanis, M.; Konstantinidis, T.; Vrioni, G.; Tsakris, A. Antimicrobial evaluation of various honey types against carbapenemase-producing Gram-negative clinical isolates. *Antibiotics* **2022**, *11*, 422.
25. Tananaki, C.; Rodopoulou, M.-A.; Dimou, M.; Kanelis, D.; Liolios, V. The total phenolic content and antioxidant activity of nine monofloral honey types. *Appl. Sci.* **2024**, *14*, 4329.
26. Kędzierska-Matysek, M.; Teter, A.; Stryjecka, M.; Skałecki, P.; Domaradzki, P.; Rudaś, M.; Florek, M. Relationships linking the colour and elemental concentrations of blossom honeys with their antioxidant activity: A chemometric approach. *Agriculture* **2021**, *11*, 702.
27. Vanhanen, L.P.; Emmertz, A.; Savage, G.P. Mineral analysis of mono-floral New Zealand honey. *Food Chem.* **2011**, *128*, 236–240.
28. Drivelos, S.A.; Danezis, G.P.; Halagarda, M.; Popek, S.; Georgiou, C.A. Geographical origin and botanical type honey authentication through elemental metabolomics via chemometrics. *Food Chem.* **2021**, *338*, 127936. https://doi.org/10.1016/j.foodchem.2020.127936.
29. Lakshitha, R.; Kantono, K.; Chen, T.; Le, T.T.; Gannabathula, S.; Hamid, N. Volatile fingerprinting and interpretable machine learning for authenticating New Zealand monofloral honeys. *Food Res. Int.* **2026**, *233*, 118954. https://doi.org/10.1016/j.foodres.2026.118954.
30. Rohart, F.; Gautier, B.; Singh, A.; Lê Cao, K.-A. mixOmics: An R package for 'omics feature selection and multiple data integration. *PLoS Comput. Biol.* **2017**, *13*, e1005752.
31. Singh, A.; Shannon, C.P.; Gautier, B.; Rohart, F.; Vacher, M.; Tebbutt, S.J.; Lê Cao, K.-A. DIABLO: An integrative approach for identifying key molecular drivers from multi-omics assays. *Bioinformatics* **2019**, *35*, 3055–3062.
32. Sadowska-Bartosz, I.; Bartosz, G. Evaluation of the antioxidant capacity of food products: Methods, applications and limitations. *Processes* **2022**, *10*, 2031.
33. Apak, R.; Calokerinos, A.; Gorinstein, S.; Segundo, M.A.; Hibbert, D.B.; Gülçin, İ.; Demirci Çekiç, S.; Güçlü, K.; Özyürek, M.; Çelik, S.E. Methods to evaluate the scavenging activity of antioxidants toward reactive oxygen and nitrogen species (IUPAC Technical Report). *Pure Appl. Chem.* **2022**, *94*, 87–144.
34. Zannini, M.; Cattivelli, A.; Nissen, L.; Conte, A.; Gianotti, A.; Tagliazucchi, D. Identification, Bioaccessibility, and Antioxidant Properties of Phenolic Compounds in Carob Syrup. *Foods* **2024**, *13*, 2196. https://doi.org/10.3390/foods13142196.
35. Benkahoul, M.; Bramki, A.; Benslama, O.; Toumi, M.E.; Maghboune, I.; Varela, R.M.; Zorrilla, J.G. Phytochemical Profiling and Antioxidant Properties of *Ziziphus lotus* (L.) Fruits Supported by Xanthine Oxidase Inhibition and Molecular Docking. *Plants* **2026**, *15*, 708. https://doi.org/10.3390/plants15050708.
36. Lakhmili, H.; Warda, K.; El-Abbassi, A.; Hafidi, A. Antioxidant and anti-glycation activity of eight Moroccan honeys from different botanical origins. *Discov. Food* **2024**, *4*, 6. https://doi.org/10.1007/s44187-024-00074-y.
37. Jerković, I.; Radonić, A.; Kranjac, M.; Zekić, M.; Marijanović, Z.; Gudić, S.; Kliškić, M. Red clover (*Trifolium pratense* L.) honey: Volatiles chemical-profiling and unlocking antioxidant and anticorrosion capacity. *Chem. Pap.* **2016**, *70*, 726–736.
38. Becerril-Sánchez, A.L.; Quintero-Salazar, B.; Dublán-García, O.; Escalona-Buendía, H.B. Phenolic compounds in honey and their relationship with antioxidant activity, botanical origin, and color. *Antioxidants* **2021**, *10*, 1700.

39. Mărgăoan, R.; Topal, E.; Balkanska, R.; Yücel, B.; Oravecz, T.; Cornea-Cipcigan, M.; Vodnar, D.C. Monofloral honeys as a potential source of natural antioxidants, minerals and medicine. *Antioxidants* **2021**, *10*, 1023.
40. Pauliuc, D.; Dranca, F.; Oroian, M. Antioxidant activity, total phenolic content, individual phenolics and physicochemical parameters suitability for Romanian honey authentication. *Foods* **2020**, *9*, 306.
41. Bong, J.; Loomes, K.M.; Lin, B.; Stephens, J.M. New approach: Chemical and fluorescence profiling of NZ honeys. *Food Chem.* **2018**, *267*, 355–367.
42. Beitlich, N.; Koelling-Speer, I.; Oelschlaegel, S.; Speer, K. Differentiation of Manuka Honey from Kanuka Honey and from Jelly Bush Honey using HS-SPME-GC/MS and UHPLC-PDA-MS/MS. *J. Agric. Food Chem.* **2014**, *62*, 6435–6444. https://doi.org/10.1021/jf501818f.
43. McDonald, C.M.; Keeling, S.E.; Brewer, M.J.; Hathaway, S.C. Using chemical and DNA marker analysis to authenticate a high-value food, manuka honey. *npj Sci. Food* **2018**, *2*, 9. https://doi.org/10.1038/s41538-018-0016-6.
44. Dżugan, M.; Tomczyk, M.; Sowa, P.; Grabek-Lejko, D. Antioxidant activity as biomarker of honey variety. *Molecules* **2018**, *23*, 2069.
45. Wang, H.; Li, L.; Lin, X.; Bai, W.; Xiao, G.; Liu, G. Composition, functional properties and safety of honey: A review. *J. Sci. Food Agric.* **2023**, *103*, 6767–6779.
46. Grainger, M.N.C.; Klaus, H.; Hewitt, N.; French, A.D. Investigation of inorganic elemental content of honey from regions of North Island, New Zealand. *Food Chem.* **2021**, *361*, 130110.
47. Pavlin, A.; Kočar, D.; Imperl, J.; Kolar, M.; Marolt, G.; Petrova, P. Honey origin authentication via mineral profiling combined with chemometric approaches. *Foods* **2023**, *12*, 2826.
48. Tlak Gajger, I.; Dar, S.A.; Ahmed, M.M.M.; Aly, M.M.; Vlainić, J. Antioxidant capacity and therapeutic applications of honey: Health benefits, antimicrobial activity and food processing roles. *Antioxidants* **2025**, *14*, 959.
49. Apak, R.; Güçlü, K.; Özyürek, M.; Karademir, S.E. Novel total antioxidant capacity index for dietary polyphenols and vitamins C and E, using their cupric ion reducing capability in the presence of neocuproine: CUPRAC method. *J. Agric. Food Chem.* **2004**, *52*, 7970–7981. https://doi.org/10.1021/jf048741x.
50. Csepregi, K.; Neugart, S.; Schreiner, M.; Hideg, É. Comparative Evaluation of Total Antioxidant Capacities of Plant Polyphenols. *Molecules* **2016**, *21*, 208. https://doi.org/10.3390/molecules21020208.
51. Everette, J.D.; Bryant, Q.M.; Green, A.M.; Abbey, Y.A.; Wangila, G.W.; Walker, R.B. Thorough Study of Reactivity of Various Compound Classes toward the Folin–Ciocalteu Reagent. *J. Agric. Food Chem.* **2010**, *58*, 8139–8144. https://doi.org/10.1021/jf1005935.

Disclaimer/Publisher's Note: The statements, opinions and data contained in all publications are solely those of the individual author(s) and contributor(s) and not of MDPI and/or the editor(s). MDPI and/or the editor(s) disclaim responsibility for any injury to people or property resulting from any ideas, methods, instructions or products referred to in the content.